# Atmospheric circulation is reflected in precipitation isotope gradients over the conterminous United States

Zhongfang Liu,[1] Gabriel J. Bowen,[1,2] and Jeffrey M. Welker[3]

[1]   The stable isotopic ($\delta^{18}$O and $\delta^2$H) composition of meteoric precipitation integrates information on the history of water fluxes to, from, and between air masses as they traverse the continents. The development of new methods relating isotopic data to water cycle processes will increase our ability to understand this system and its response to natural and anthropogenic forcing. Here we present an analysis of 2 years (1992–1993) of precipitation isotope data from 73 sites across the conterminous United States. We focus on patterns in the spatial precipitation isotope gradients (rate and direction of isotopic change in space), a metric which we suggest reflects two factors: (1) variation in the balance of rainout and land-surface recycling for air masses moving across the continent and (2) the spatial juxtaposition of air masses carrying moisture of differing origin and rainout history (e.g., Pacific versus Gulf of Mexico moisture). We demonstrate that the position of zones of particularly high precipitation isotope slopes correspond to the time-averaged position of air mass boundaries and to regions where prevailing moisture transport trajectories interact with orographic barriers. Differences in the location of high-slope zones between winter and summer seasons and between the same seasons in 1992 and 1993 can be related to differences in circulation and weather patterns. These results suggest new opportunities for the interpretation of precipitation, vapor, and paleoclimate water isotope data in the context of regional climate dynamics through spatial analysis.

**Citation:**  Liu, Z., G. J. Bowen, and J. M. Welker (2010), Atmospheric circulation is reflected in precipitation isotope gradients over the conterminous United States, *J. Geophys. Res.*, *115*, D22120, doi:10.1029/2010JD014175.

## 1.   Introduction

[2]   The stable isotope ($\delta^{18}$O and $\delta^2$H) composition of meteoric precipitation reflects spatial and temporal variation in climate on a variety of scales. Such variations are preserved in authigenic minerals and organic compounds and represent excellent archives for interpreting past continental climate change. In the past decades, numerous paleorecords have been investigated for reconstructing Pleistocene/Holocene climate change across the continental United States, including lacustrine sediments [e.g., *Yu and Eicher*, 1998; *Anderson et al.*, 2001; *Schwalb and Dean*, 2002], speleothems [e.g., *Dorale et al.*, 1992, 1998] and plant cellulose [e.g., *Feng et al.*, 2007]. The majority of this work has used isotopic data as an indirect proxy for local climate variables (e.g., temperature or precipitation amount) based on modern empirical isotope/climate correlations [e.g., *Wright and Leavitt*, 2006].

[3]   The isotopic composition of meteoric precipitation is also closely related to atmospheric circulation patterns through their effect on the sources and transport paths of atmospheric vapor across the continents [e.g., *Lawrence et al.*, 1982; *Friedman et al.*, 2002a]. In many cases, recognition of past changes in atmospheric circulation is critical to developing dynamical understanding of paleoclimatic change and its effects on continental environments [e.g., *Smith and Hollander*, 1999]. An increasing number of studies attempt to relate isotope records to dynamical climate modes and synoptic features of the atmospheric circulation [*Amundson et al.*, 1996; *Yu et al.*, 1997; *Smith and Hollander*, 1999; *Feng et al.*, 2007], a potentially powerful approach for reconstructing the large-scale state of climate. Such analyses require a new understanding of the modern isotopic expression of climate modes and synoptic features in order to support robust interpretations of isotopic archive data [*Baldini et al.*, 2008].

[4]   Information on the relationship between precipitation isotopic composition and modern atmospheric circulation in the United States has been derived from short-term sampling conducted by individual research groups, long-term monitoring data collected by the International Atomic Energy Agency's Global Network for Isotopes in Precipitation (GNIP), and, more recently, the national-scale United States Network for Isotopes in Precipitation (USNIP) [*Welker*, 2000; *Dutton et al.*, 2005; *Vachon et al.*, 2007]. Isotopic vari-

---

[1]Department of Earth and Atmospheric Sciences, Purdue University, West Lafayette, Indiana, USA.
[2]Purdue Climate Change Research Center, Purdue University, West Lafayette, Indiana, USA.
[3]Environment and Natural Resources Institute, University of Alaska Anchorage, Anchorage, Alaska, USA.

ation across the contiguous United States exhibits strong continentality, with $\delta^2H$ and $\delta^{18}O$ values decreasing from the coasts to the continental interior along dominant circulation trajectories in response to temperature-, convective- and front-driven rainout of $^2H$- and $^{18}O$- enriched precipitation. Working in the western United States, *Ingraham and Taylor* [1991] demonstrated that changes in the rates of isotopic change with distance along circulation trajectories could be attributed to variation in the relative rates of rainout and resupply of water to the atmosphere through evapotranspiration. As a result of differences in rainout rates, differences in the overland path length, and differences in vapor source-region conditions, air masses arriving at a given location via different circulation trajectories often carry moisture with very different isotopic composition. For example, there are significant differences in the $\delta^2H$ and $\delta^{18}O$ values of moisture reaching the Great Basin via transport from the North Pacific, subtropical Pacific, Gulf of California, and Gulf of Mexico, with lower values corresponding to precipitation events derived from the more northerly sources [*Friedman et al.*, 2002a]. A similar pattern has been observed for winter precipitation in upstate New York derived from North Atlantic, central Atlantic, and Arctic air masses, and in this system the deuterium excess value ($d = \delta^2H - 8 \times \delta^{18}O$, a tracer of vapor source region conditions) of precipitation also varies between air masses that have interacted with the Great Lakes (high $d$) and those that have not [*Lawrence et al.*, 1982; *Burnett et al.*, 2004]. Regional variation in time-averaged precipitation isotopic composition in several parts of the contiguous United States has been attributed in part to geographic variation in the relative amounts of water sourced via different atmospheric trajectories, for example, annual average precipitation isotope ratios are lower at sites in the southwest United States that do not receive appreciable summer monsoon precipitation, and low isotope ratios of Vermont precipitation have been associated with time periods when Arctic-derived precipitation is relatively abundant [*Friedman et al.*, 2002b; *Sjostrom and Welker*, 2009].

[5] Despite the recognition of the widespread influence of circulation on meteoric water isotope ratios, existing methods for extracting information on circulation patterns from isotope data are largely limited to the analysis of specific systems based on empirically observed isotope/circulation relationships [e.g., *Baldini et al.*, 2008; *Yoshimura et al.*, 2008; *Birks and Edwards*, 2009]. Here we introduce and test the hypothesis that the juxtaposition of moisture with different sources, rainout history, and isotopic composition along boundaries in the synoptic circulation should be reflected in the spatial gradient (slope $- \Delta\delta^{18}O/\Delta$distance $-$ and aspect) of precipitation isotopic composition. Because large-scale, synoptic data on atmospheric water isotope ratios do not yet exist, we test the hypothesis by examining the relationship between time-averaged (seasonal) circulation patterns and precipitation isotopic gradients calculated from two years of monitoring data for the contiguous United States. Our analysis demonstrates robust correspondence between the isotopic gradient and atmospheric circulation that would not be clearly apparent based on raw isotopic data from individual stations or sampling networks. In contrast to previous techniques, which are applied to a single region (e.g., circulation controls over an ice core site) or assume a circu-

lation control (e.g., North Atlantic Oscillation) a priori and then look for its isotopic expression over a large area, this technique allows different possible circulation controls over a large area to emerge empirically from the isotope data. As analytical advances and coordinated monitoring efforts lead to modern and paleowater proxy data sets that are denser in spatial and temporal resolution, the gradient analysis introduced here will represent a powerful approach to elucidating large-scale processes in the water cycle and their change over time.

## 2. Data and Methods

[6] We analyzed data generated as part of the USNIP (United States Network for Isotopes in Precipitation) program [*Welker*, 2000] representing more than 3400 precipitation samples collected weekly at 73 sites across the conterminous United States for 1992 and 1993. The data include $\delta^{18}O$ values (reported in $\delta$ notation and per mil units relative to Vienna Standard Mean Ocean Water, or VSMOW, standard) and corresponding precipitation amount. Raw weekly values were used to calculate precipitation-amount weighted isotope ratios for the summer (June, July, and August) and winter (January and February; December data were not used because the available isotopic record spanned January 1992 to December 1993) seasons of each study year.

[7] Interpolated maps of precipitation $\delta^{18}O$ values were produced at a resolution of 2.5 arcmin with Ordinary Kriging [*Moyeed and Papritz*, 2002] in ArcGIS 9.2 using a spherical semivariogram model with nugget (all interpolations were conducted using the Geostatistical Analyst extension). Gradient and aspect (direction of steepest descent) were calculated for the resulting fields using the Slope and Aspect tools in the Spatial Analyst extension. Because we were interested in the reflection of large-scale (i.e., >100 km) features of the atmospheric circulation in the observational data, we chose to conduct the interpolation without the use of ancillary variables such as elevation [*Bowen and Wilkinson*, 2002] that would introduce high-amplitude variability in the interpolated surface over short length scales.

[8] We compared the spatial precipitation $\delta^{18}O$ gradients with climate fields representing sea level pressure (SLP), mean surface air temperature and moisture flux obtained from the NCEP/NCAR reanalysis data set (available at http://www.cdc.noaa.gov/data/gridded/data.ncep.reanalysis.html), as well as precipitation amount obtained from Global Precipitation Climatology Project (GPCP, available at http://jisao.washington.edu/data/gpcp). Surface temperature spatial slopes were calculated from the reanalysis grids using the same methods applied to the isotopic grids. We also provide a direct comparison with air mass distributions using Spatial Synoptic Classification (SSC) [*Kalkstein et al.*, 1996] data (available at http://sheridan.geog.kent.edu/ssc.html). The SSC is a semiautomatic classification scheme that identifies six different weather types (dry polar, dry temperate, dry tropical, moist polar, moist temperate and moist tropical) across the North American continent based on four-time-daily observations of temperature, dew point, wind, pressure and cloud cover at an individual site. A detailed description of SSC system is given by *Sheridan* [2002]. For our analysis, we considered primarily the dry polar, moist moderate,
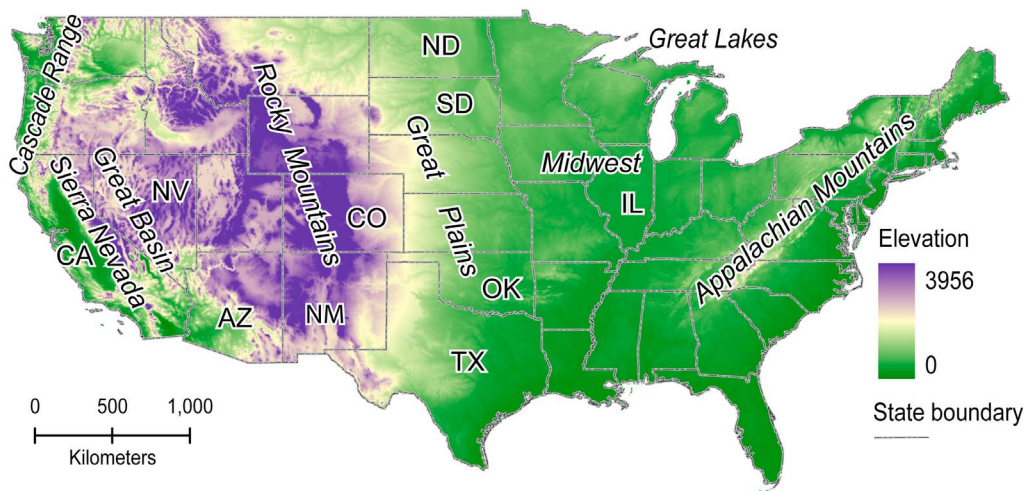
**Figure 1.** Locations of the physiographic provinces (italicized) and states discussed in the text. The background color field represents land surface elevation (meters) from the United States Geological Survey (USGS) GTOPO30 digital elevation model (http://eros.usgs.gov/#/Find_Data/Products_and_Data_Available/gtopo30_info). AZ, Arizona; CA, California; CO, Colorado; IL, Illinois; ND, North Dakota; NM, New Mexico; NV, Nevada; OK, Oklahoma; SD, South Dakota; TX, Texas.

and moist tropical air mass classes, as these represent the contrasting influence of polar, midlatitude oceanic, and tropical oceanic air masses most likely to provide vapor of contrasting isotopic composition to the continental interior. As an additional proxy for water vapor source history, we also calculated and mapped the spatial distribution of deuterium excess using the same ordinary kriging method applied to the isotope ratio data.

## 3. Climatological Setting

[9] The hydroclimate of the contiguous United States is dominated by the competing influence of three distinct air masses that originate over the Pacific Ocean, Gulf of Mexico/subtropical Atlantic and the Arctic [*Bryson and Hare*, 1974]. The relative influence of each air mass varies spatially and temporally. During summer months, monsoonal moisture from the Gulf of Mexico and subtropical Atlantic dominate most of the contiguous United States east of the Rocky Mountain Front and contribute lesser amounts of water to the southwestern states. Pacific sources contribute moisture in the Pacific Northwest (North Pacific air masses) and southwest (Gulf of California/subtropical Pacific air masses), whereas Arctic systems exert only a minor influence on the northernmost interior states [*Bryson and Hare*, 1974]. During the winter, southward displacement of the jet stream and establishment of high pressure over the continental interior lead to increased dominance of moist Pacific air masses across the western United States. Anticyclonic flow around continental high-pressure systems brings dry Arctic air masses deep into the middle of the continental United States, producing frontal storm systems that severely limit the propagation of Gulf of Mexico and Atlantic moisture into the continental interior [*Maglaras et al.*, 1995]. During both seasons, secondary vapor sources such as continental evapotranspiration [e.g., *Ingraham and Taylor*, 1991] and evaporation from the Great Lakes [*Gat et al.*, 1994; *Niziol*

*et al.*, 1995; *Burnett et al.*, 2004] contribute additional moisture within some regions.

[10] Reanalysis data for 1992 and 1993 demonstrate substantial differences in circulation patterns and hydroclimatology for these two years. Relative to 1992, the summer of 1993 featured intensified low pressure over the western Great Plains and a steeper pressure gradient between the subtropical Atlantic and the continental interior (Figures 1 and 2), leading to unusually strong transport of moisture from the Gulf of Mexico to the northern Great Plains states (Figures 1 and 3) and correspondingly high summer rainfall in this region (Figure 4).

[11] For the winter months, there was a substantial difference in the geographic location of the primary high pressure for the two study years, with a strong high centered over the Rocky Mountain interior during the winter of 1992 and a more diffuse high-pressure system situated over the northern Great Plains during 1993 (Figures 1–3). During 1992, the west-shifted high blocked westerly storms and reduced moisture transport from the Pacific to the southwest and western interior, producing a relatively dry winter in this region (Figures 3 and 4). East of the Rocky Mountains, the lack of a strong high over the Great Plains during 1992 reduced the occurrence of strong frontal storm systems and cyclonic moisture transport from the Gulf and Atlantic into the continental interior. This led to lower winter precipitation amounts in the Midwest and a relatively wet winter in the Gulf Coast, particularly in Texas (Figures 1 and 4). In 1993, higher precipitation amounts extend east from the central Great Plains to the Atlantic Coast, suggesting stronger precipitation from frontal systems in this region.

## 4. Results

### 4.1. Precipitation $\delta^{18}O$ Patterns

[12] Precipitation $\delta^{18}O$ values exhibit significant spatial autocorrelation for all time periods studied (Moran's I >
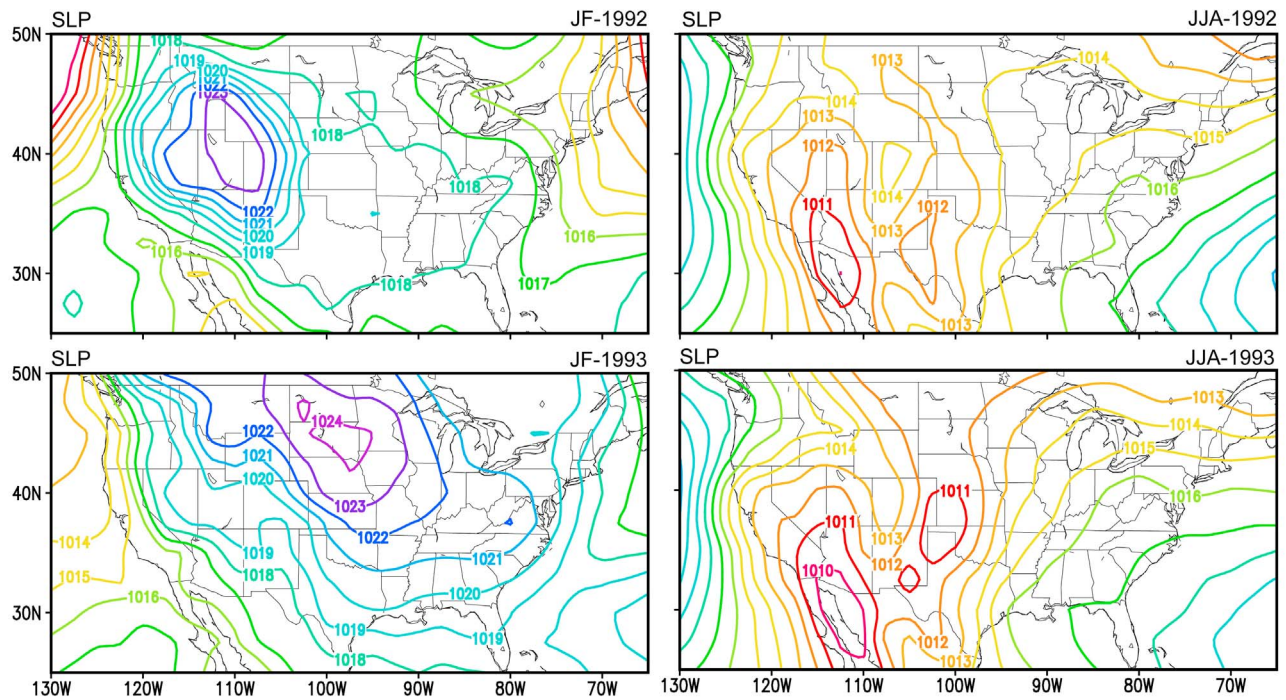
**Figure 2.** Sea level pressure fields (SLP) for winter (JF) and summer (JJA) of 1992 and 1993, calculated from the NCAR/NCEP reanalysis data. The contour interval is 1 mbar.
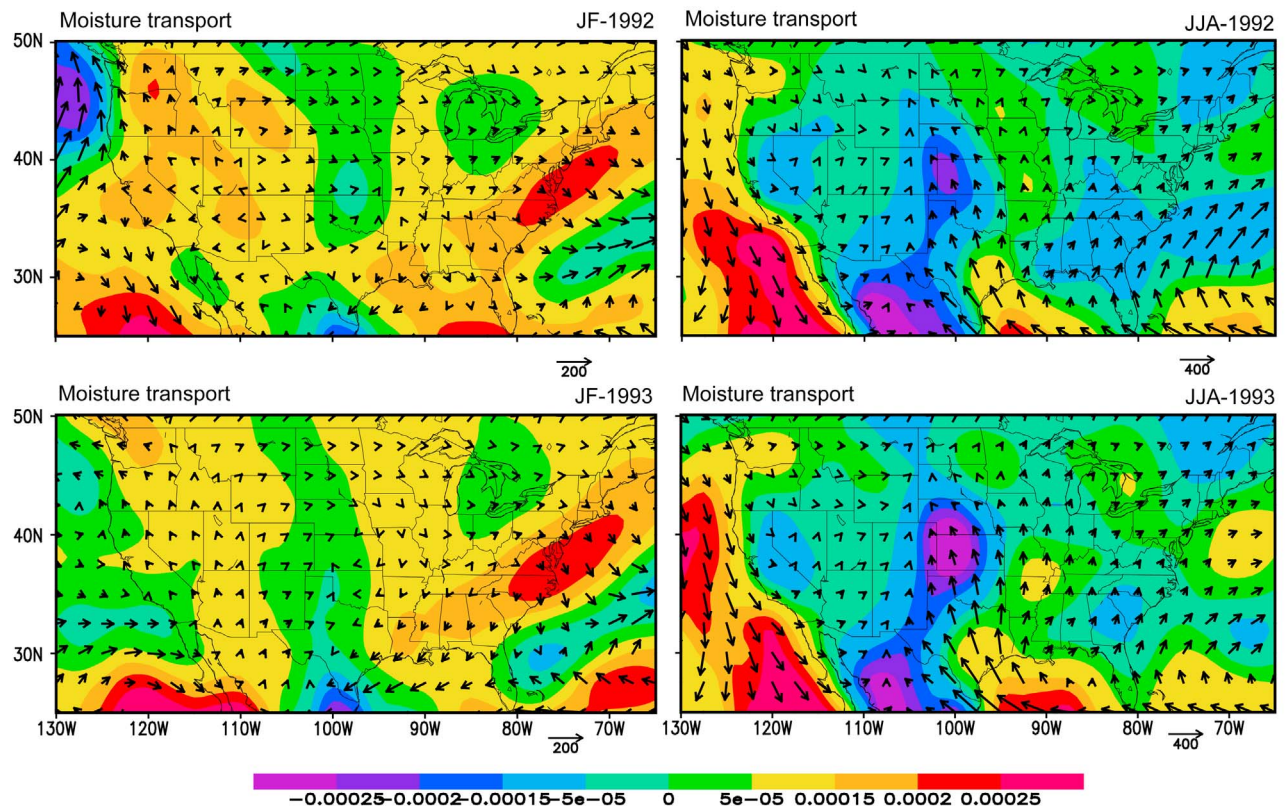


**Figure 3.** Vertically integrated moisture transport for 1000–700 hPa levels for winter (JF) and summer (JJA) of 1992 and 1993, calculated from the NCAR/NCEP reanalysis data. The arrow denotes vertically integrated moisture flux (kg m$^{-1}$ s$^{-1}$) and the color fields denote moisture flux divergence (kg m$^{-2}$ s$^{-1}$).
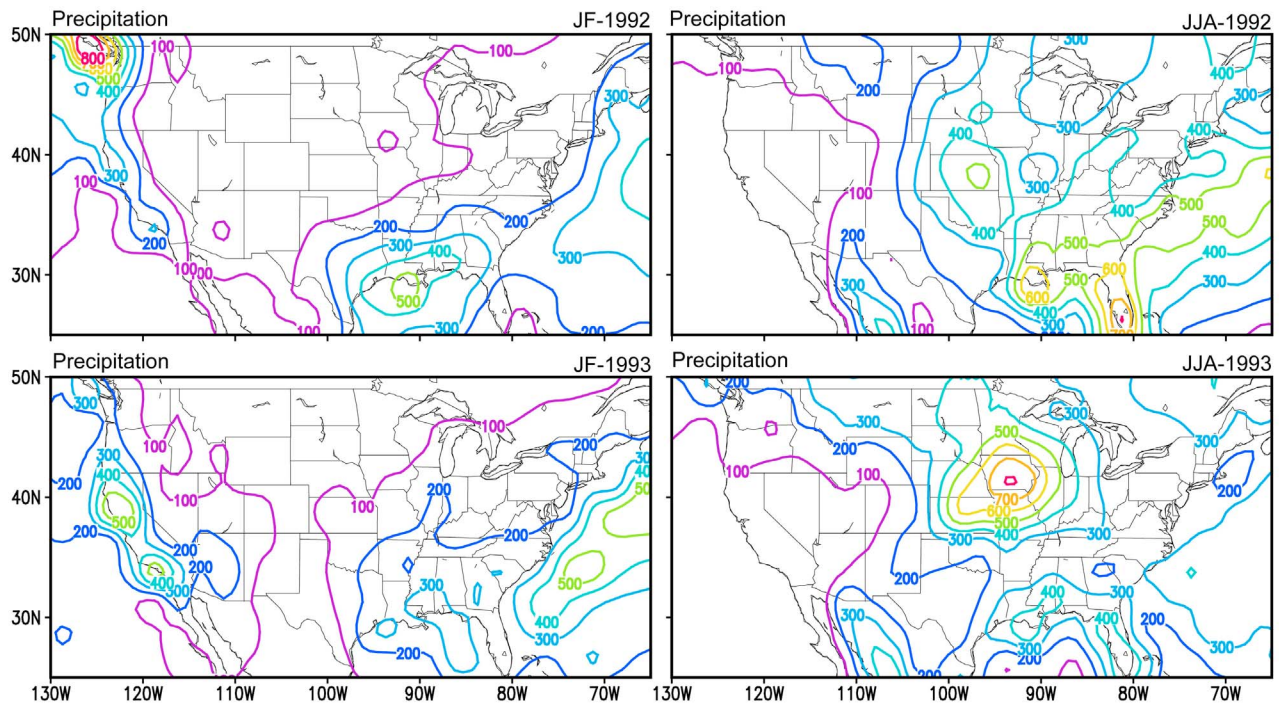
**Figure 4.** Mean surface precipitation fields for winter (JF) and summer (JJA) of 1992 and 1993, calculated from Global Precipitation Climatology Project [*Adler et al.*, 2003] monthly precipitation data. The contour interval is 100 mm.

0.17; Z > 8.9; *p* < 0.01). The semivariogram model range varied from 2509 to 4128 km, suggesting that the interpolation was capturing spatial patterns at scales of hundreds to thousands of kilometers over which patterns of atmospheric circulation might be expressed. A nonzero nugget value was fit for each data set, indicating that local-scale variation existed in the data that could not be represented in the kriged surface. Root-mean-square error (RMSE) values for the interpolated surface, determined through cross validation within Geostatistical Analyst, are lower for the summer months (1.5‰ and 1.9‰ for 1992 and 1993, respectively) and higher for winter (3.0‰ and 2.8‰). These values are roughly proportional to the standard deviation of station $\delta^{18}O$ values for each study period (2.9‰ and 3.9‰ for summer 1992 and 1993, and 5.4‰ for both winters).

[13] Interpolated amount-weighted average $\delta^{18}O$ values accurately reproduce the large-scale patterns described by the station data, although local deviations between station and gridded values are apparent in some cases (Figure 5). The precipitation isotope ratio maps show similar large-scale spatial patterns for summer (JJA) and winter (JF) of 1992 and 1993, with values decreasing from the low-latitude, low-elevation coastal regions toward high-latitude, mountains and inland regions. The $\delta^{18}O$ values of winter precipitation span a larger range than summer precipitation, averaging −12.4‰, with a standard deviation of 4.1‰, in 1992, and −13.0‰, with a standard deviation of 4.7‰ in 1993. Summer season values are significantly higher and less variable (mean = −7.2‰ and $\sigma$ = 2.4‰ in 1992; mean = −7.5‰ and $\sigma$ = 3.3‰ in 1993). During both years, minimum values occur throughout the northern Rocky Mountains during the summer and from the northern Rockies across the northern Great

Plains in the winter. Maximum values occur along the Gulf Coast during all time periods.

## 4.2. Patterns of Precipitation $\delta^{18}O$ Gradients

[14] Spatial aspect values for precipitation isotope gradients are broadly similar during each time period, with northward directions on average and deflection toward the Rocky Mountain interior within the western states (Figure 6). In contrast, slope values show strong spatial and temporal variation. The $\delta^{18}O$ slopes for winter precipitation are larger (mean = 0.70‰/100 km for 1992 and 0.75‰/100 km for 1993) and more variable ($\sigma$ = 0.24‰/100 km for 1992 and 0.30‰/100 km for 1993) than those for summer (mean = 0.35‰/100 km for 1992 and 0.41‰/100 km for 1993; $\sigma$ = 0.18‰/100 km for 1992 and 0.14‰/100 km for 1993) (Figure 7). The $\delta^{18}O$ slopes reported here are close to those documented by [*Welker*, 2000] for a rainout transect in the Pacific Northwest (1.2‰/100 km) and [*Rozanski et al.*, 1993] for a transects in Europe-Eurasia (0.18‰/100 km), and South America (0.30‰/100 km).

[15] The dominant feature in the isotope gradients for the summer season is a zone of high $\delta^{18}O$ slope (large change in $\delta^{18}O$ value over a short distance) located in the midcontinent (Figure 6). This feature is approximately north-south oriented and centered on the eastern front of the Rocky Mountains, but the details of its geometry and geographic location differ among the two study years. During 1992, the high-slope zone extends in a WSW-ENE direction across Arizona and New Mexico before curving northward along the ∼103−105th meridian to the Dakotas, and deflecting eastward to Great Lakes. In contrast, in 1993 the zone trends from the SSE to NNW across west Texas and Oklahoma
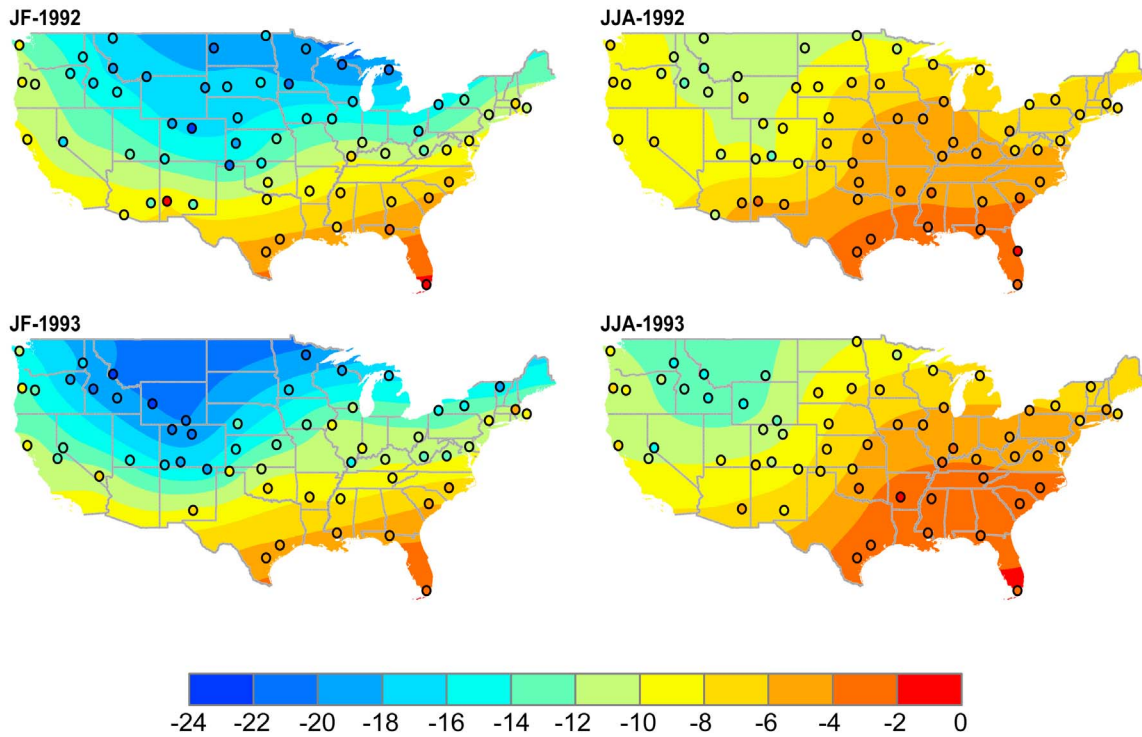
**Figure 5.** Spatial distribution of precipitation $\delta^{18}O$ for winter (JF) and summer (JJA) of 1992 and 1993. Colored points denote $\delta^{18}O$ value of individual data collection sites, and color fields denote spatial patterns generated from ordinary kriging interpolation. All values are in ‰ units.

and extends northward along the ~103–105th meridian all the way to the Canadian border. During 1992 the $\delta^{18}O$ slopes are slightly steeper in the south than the north, and the reverse condition occurs in 1993. Secondary zones of moderately high $\delta^{18}O$ slopes occur in vicinity of the Great Lakes and the Cascades.

[16] Winter patterns of precipitation $\delta^{18}O$ slopes are distinctly different from those seen during summer months. A
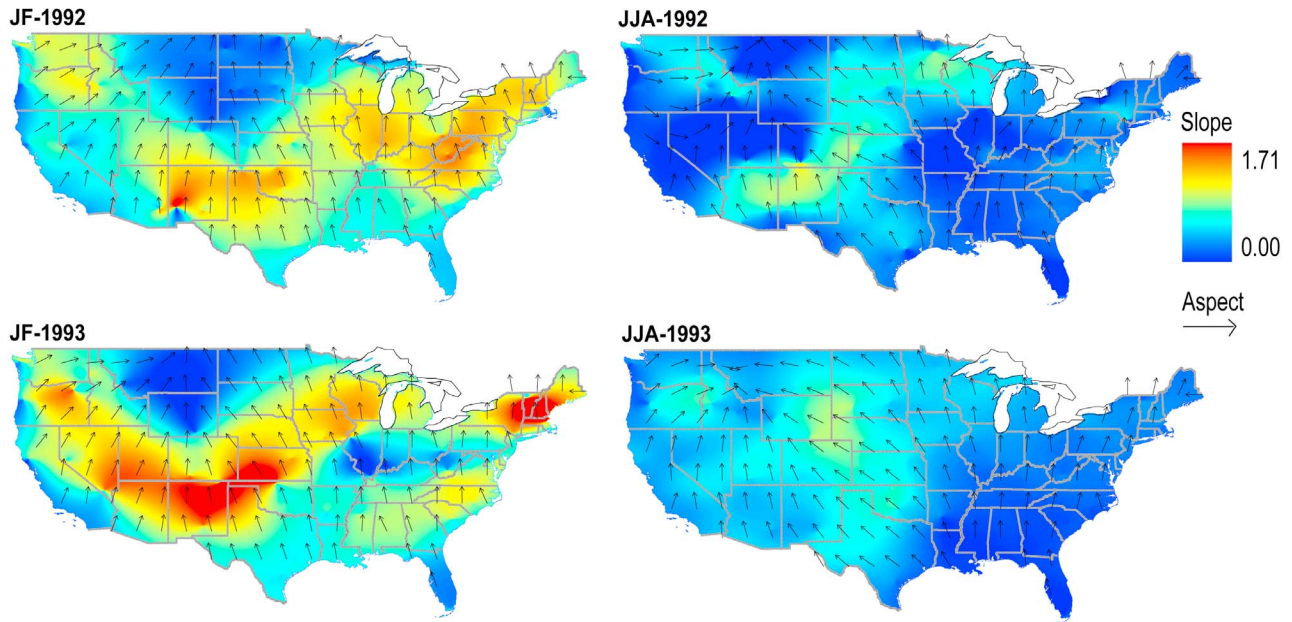


**Figure 6.** Slope and aspect of the precipitation $\delta^{18}O$ gradient for winter (JF) and summer (JJA) of 1992 and 1993. Background color fields and arrows denote gradient and aspect, respectively. All values are in units of ‰/100 km.
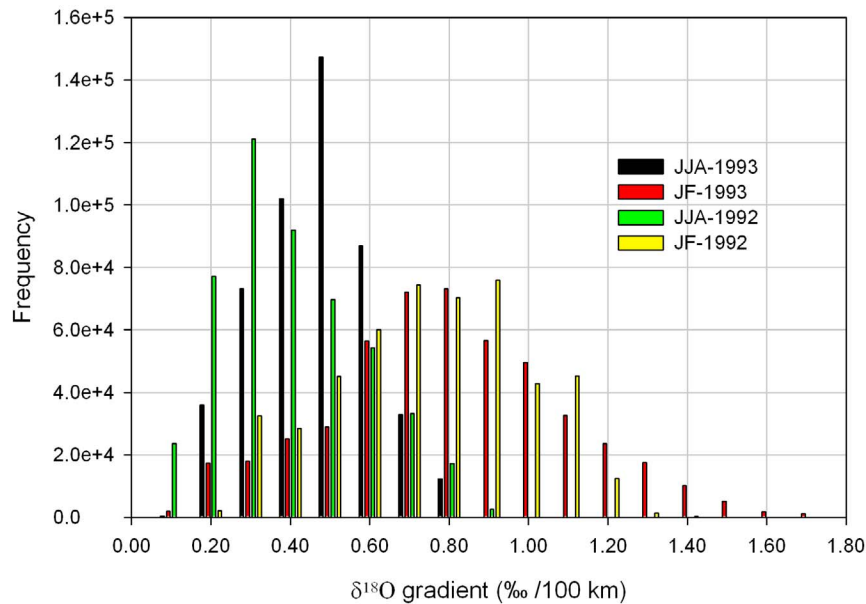
**Figure 7.** Frequency distribution for precipitation $\delta^{18}$O slope values for winter (JF) and summer (JJA) of 1992 and 1993.

zone of high $\delta^{18}$O slopes envelopes the Rocky Mountains and northern Great Plains in the form of "U"-shaped band, extending southeast from the Cascades through Nevada to New Mexico (Figures 1 and 6). From there, strong $\delta^{18}$O slopes curve northeastward across the Great Plains to the Great Lakes region. Differences in this pattern are evident between the two study years in the Sierra Nevada, where slopes during the winter of 1992 are much lower than in 1993, and in the Great Plains, where the high-slope zone is somewhat stronger and positioned farther to the north during 1993. A secondary zone of relative high $\delta^{18}$O slope, which is much stronger in 1992 than in 1993, exists across the Great Lakes and north Atlantic Coast regions.

[17] We know of no analytical expression for the uncertainty of mapped $\delta^{18}$O gradients presented here. Although the analysis presented in section 4.1 demonstrates that the interpolated $\delta^{18}$O values from which the gradients are calculated have significant uncertainty associated with them, the attribution and interpretation of this error is uncertain (e.g., as a product of data error, such as sampling and analysis errors, versus a reflection of real variation in $\delta^{18}$O values over small scales). As a result, error estimation would likely be best achieved through a nonparametric numerical (e.g., Monte Carlo) method, which is beyond the scope of this manuscript. Although such work should be pursued, we believe there is strong evidence that the large-scale patterns discussed here are robust. All features of the $\delta^{18}$O gradient we discuss are spatially continuous and defined by data from many adjacent measurement stations, implying that they are not artifacts of single errant data values. For each map, a single spatial semivariogram model was used across the entire map domain, and visual inspection suggests that the spatial distribution of gradient values is not directly related to the spatial distribution (i.e., spacing) of stations, implying that the observed patterns are not an artifact of interpolation

model. Last, the broad similarity of the observed seasonal patterns across 2 years of data, analyzed independently, lends support to the interpretation that the patterns are robust features of the precipitation isotope climatology.

### 4.3. Patterns of Precipitation Deuterium Excess

[18] Spatial patterns of deuterium excess ($d$) values across the contiguous United States vary both among summer and winter seasons and among years (Figure 8). In contrast with precipitation $\delta^{18}$O values and gradients, the $d$ values show significant but relatively weak spatial autocorrelation (Moran's Index > 0.05; Z > 3.6; p < 0.01), except for the winter of 1993, when $d$ values were not spatially autocorrelated (Moran's Index = −0.04; Z > −1.3). In the summer, the $d$ values tend to have a sharp division between the eastern and western United States. For summer of 1992, $d$ values of less than 8‰ dominate the continent to the north and west of an arc extending from the northern Great Lakes to the SW, across the central Rocky Mountains, and into the Pacific Northwest, with higher values found elsewhere. In 1993 this line dividing high and low $d$ values is oriented N-S along the ~103–105th meridian, with low $d$ values found across the western half of the country. Winter precipitation had slightly larger $d$ values on average, and the spatial distribution of $d$ is comparatively complex. During all years and seasons, the highest $d$ values (>15‰) occur in the northeastern states.

## 5.  Discussion

### 5.1.  Orographic Effect

[19] Decreases in precipitation isotope ratios as air masses are lifted over high topography in the western United States are well documented [e.g., *Ingraham et al.*, 1991; *Dutton et al.*, 2005]. In several cases, zones of high-precipitation
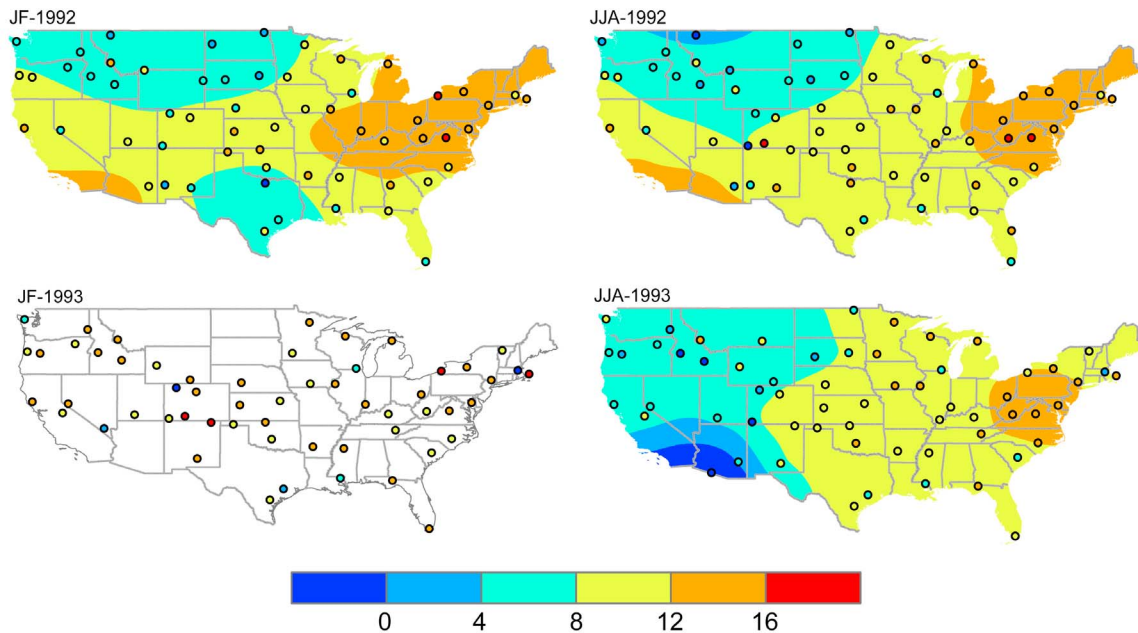
**Figure 8.** Spatial distribution of precipitation deuterium excess values for the winter (JF) and summer (JJA) of 1992 and 1993. Values for individual data collection sites are shown as colored points, and the background color fields show spatial patterns of *d* values (except for the winter of 1993, for which *d* values were not spatially autocorrelated) interpolated by ordinary kriging. All values are in units of ‰.

isotope slopes identified on our gradient map (Figure 6) are approximately colocated with known regions of strong orographic rainout (e.g., maxima over the Cascades, summer maxima in the vicinity of the Rocky Mountain Front), suggesting that the interaction of high topography with the prevailing circulation determines the geographic location of these high-slope zones. The gradient maps, however, demonstrate that these features are not static, and vary over time in response to variation in atmospheric circulation. In the west coast region, the high-slope zone tends to be stronger and more clearly defined in the winter season, and during both seasons the feature is notably weaker across California and Nevada during 1992 than 1993 (see section 5). In the summer season, high-slope values are situated along parts of the Rocky Mountain Front, but the location of maximum slope values shifts between more southerly and northerly positions in 1992 and 1993, respectively. In the eastern United States, relatively high slopes are observed in the vicinity of the Appalachian Mountains during some time periods, in particular during the winter of 1992, which may in part reflect orographic effects.

### 5.2. Temperature Effect

[20] Patterns of precipitation isotope ratio variation across the contiguous United States closely parallel those of temperature, with regions of low temperature being characterized by low $\delta^{18}$O values (Figure 5) [*Harvey and Welker*, 2000; *Dutton et al.*, 2005; *Bowen*, 2008]. The importance of temperature-driven rainout in governing spatial patterns of isotopic change can be seen through the pair-wise comparison of seasonal temperatures and precipitation isotope ratios for monitoring stations (Figure 9). Isotopic differences between stations separated by 1500 km or less are well cor-

related with differences in temperature, with slope values of 0.38 to 0.64‰ °C$^{-1}$ and $R^2$ values of 0.42 to 0.68. These $\delta^{18}$O/temperature slopes compare well with values of 0.26 to 0.69‰ °C$^{-1}$ reported for North America, but the $R^2$ values are low relative to previous studies (ranging from 0.68 to 0.97) [*Joussaume and Jouzel*, 1993; *Harvey and Welker*, 2000].

[21] We also calculated the approximate slopes expected for these relationships if they were a pure function of temperature-driven rainout using the Rayleigh equation

$$R = R_i f^{(\alpha-1)},$$

where $R$ and $R_i$ are $^{18}$O/$^{16}$O ratio of the remaining water vapor and its initial value, respectively. The fraction of the water vapor remaining ($f$) is determined by the change in saturation vapor pressure of water, with an exponential dependence on temperature, and $\alpha$ is the temperature-dependent equilibrium liquid-vapor isotope ratio fractionation. In order to approximate the mean conditions for each of the four study periods, $\Delta\delta^{18}$O/$\Delta T$ slopes were estimated using $\alpha$ for the average station temperature ($T_a$) and calculating $f$ as the ratio of saturation vapor pressure at $T_a - 15$ to that at $T_a$. The observed $\Delta\delta^{18}$O/$\Delta T$ slopes are similar to, but in all cases lower than, the theoretical ones, and together with large scatter of observed values are consistent with the large body of literature that has demonstrated the importance of nontemperature effects, such as variation in moisture sources, transport trajectories and recycling from the landscape [*Rozanski et al.*, 1992; *Fricke and O'Neil*, 1999; *Kohn and Welker*, 2005] on controlling spatial precipitation isotope ratio distributions.
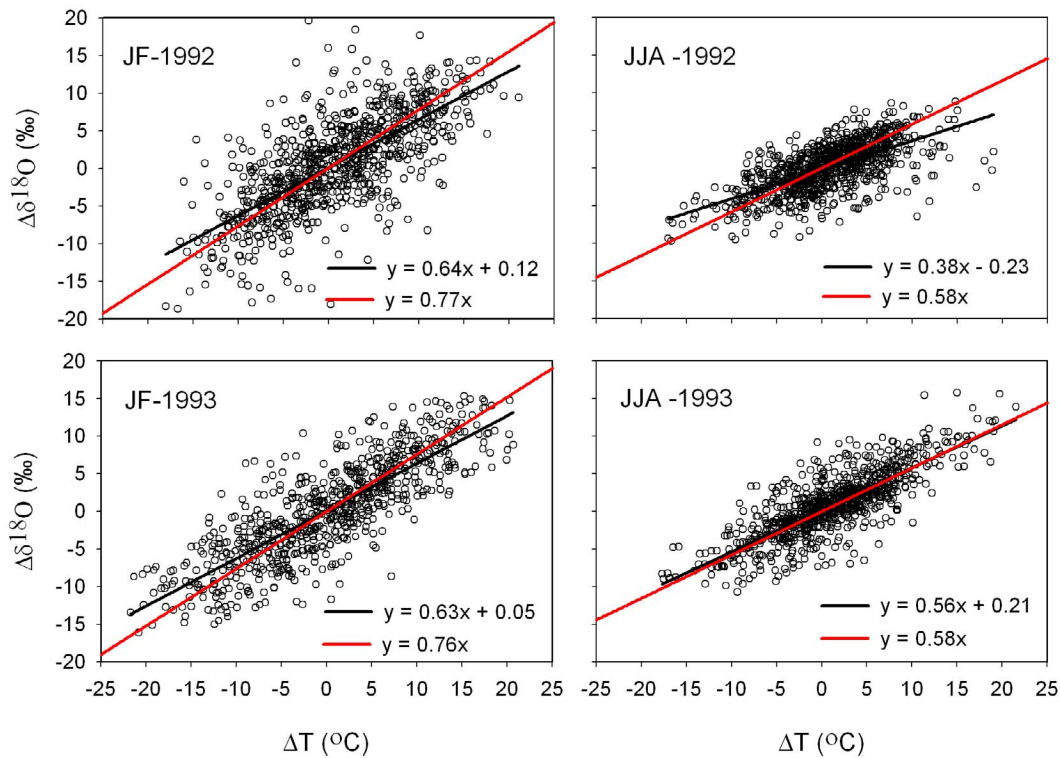
**Figure 9.** Pairwise $\delta^{18}O$ and temperature difference between precipitation monitoring sites (for all site pairs separated by <1500 km) for winter (JF) and summer (JJA) of 1992 and 1993. Black lines indicate the slope of observed $\Delta\delta^{18}O/\Delta T$ relations, and red lines indicate the slope of modeled $\Delta\delta^{18}O/\Delta T$ relations for temperature-driven Rayleigh fractionation.

[22] Although spatial variation in temperature clearly influences the large-scale pattern of precipitation isotope ratio variation, comparison of the spatial slopes of seasonal temperature distributions (Figure 10) with the precipitation isotope ratio gradient maps (Figure 6) suggests that the pattern of isotope slopes is only weakly related to temperature distributions. Rayleigh theory predicts that the rate of temperature-driven isotopic change over space would be approximately proportional to the rate of temperature change. In other words, zones of high-precipitation isotope slopes should correspond to zones of strong spatial gradients in temperature. This is clearly so in some cases: for example high-precipitation isotope slopes are colocated with strong temperature gradients in the southern Rockies during most of the study periods. The relationship is inconsistent, however: high-precipitation isotope slopes occur across parts of the Great Plains during all periods despite the absence of particularly strong temperature gradients. Conversely, strong temperature gradients in the Pacific Coast States during the winter of 1992 are not accompanied by high-precipitation isotope slopes. Although variation in spatial temperature gradients may influence the pattern of precipitation isotope slopes, they appear not to be the only, or perhaps even the primary, control on this pattern.

### 5.3. Atmospheric Circulation Controls

[23] The $\delta^{18}O$ slope fields display a number of relationships with atmospheric pressure fields, precipitation fields

and moisture transport patterns (Figures 2–4) that suggest zones of high spatial slope may be related to features of the atmospheric circulation and moisture transport. In particular, strong zones of high $\delta^{18}O$ slope dissect the midcontinent during all years and seasons in the vicinity of features of the atmospheric circulation that govern the extent of penetration of Gulf and Pacific moisture into the continental interior. We suggest that these high-slope zones correspond to the time-average position of boundaries between regions dominated by moisture from these sources and the minor arctic and continental sources.

[24] During summer, low-pressure systems in the midcontinent drive northward transport of moisture from the Gulf of Mexico and convergence of Gulf- and Pacific-sourced moisture in the vicinity of the Rocky Mountain Front (Figure 3). This boundary is approximately colocated with the dominant summer season zone of high $\delta^{18}O$ slopes, suggesting that the isotope slopes may reflect the spatial juxtaposition of the relatively ^{18}O-enriched Gulf moisture and ^{18}O-depleted Pacific moisture in this region. Perhaps the strongest evidence for the relationship between the high isotope slope zone and the penetration of Gulf moisture into the midcontinent comes from comparison of summer season precipitation and air mass frequency patterns for the summer of 1992 and 1993. In 1993, stronger and more northward-situated low pressure increased the penetration of Gulf-derived moisture into the upper Midwest and northern Great Plains relative to the summer of 1992, as reflected
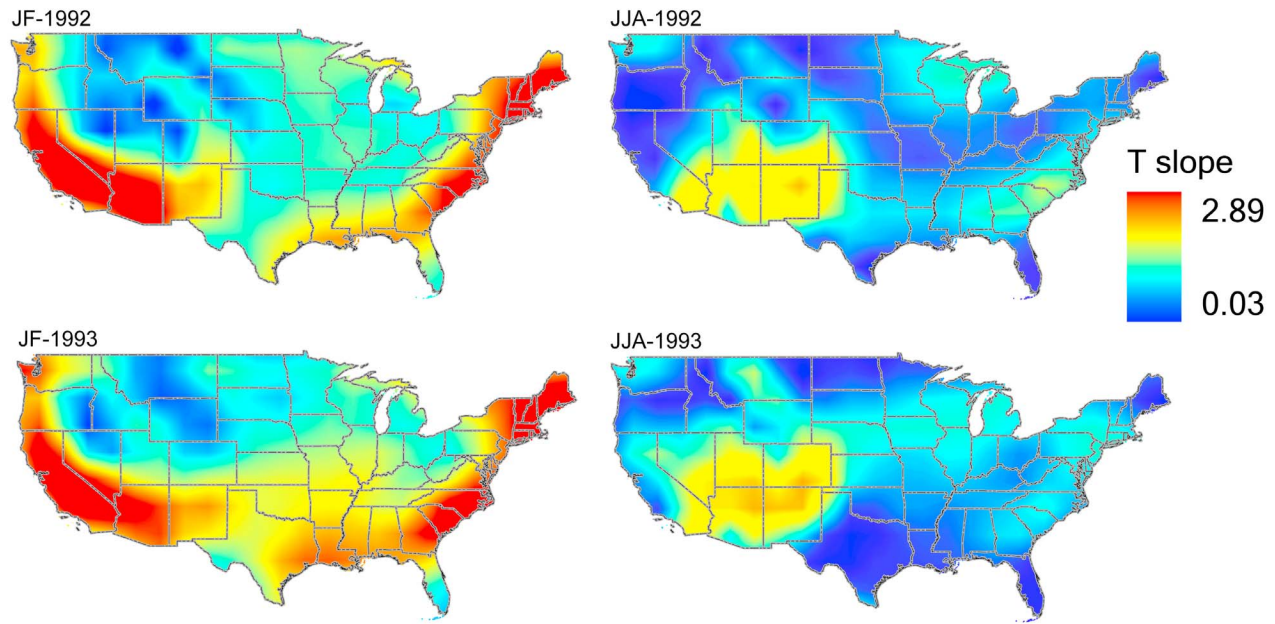
**Figure 10.** Spatial gradient (slope) fields for mean surface air temperatures in winter (JF) and summer (JJA) of 1992 and 1993, calculated from the monthly mean NCAR/NCEP reanalysis data. All values are in units of °C/100 km.

by northward-displaced contours of moist tropical (MT) air mass frequency and precipitation-amount contour in the Great Plains (Figures 4 and 11). In each year, the high $\delta^{18}O$ slope zone approximately parallels the northern and western

extent of MT air mass influence and corresponding high precipitation amounts, extending northward and westward to the Canadian border in 1993 and cutting to the northeast across the northern Great Plains in 1992.
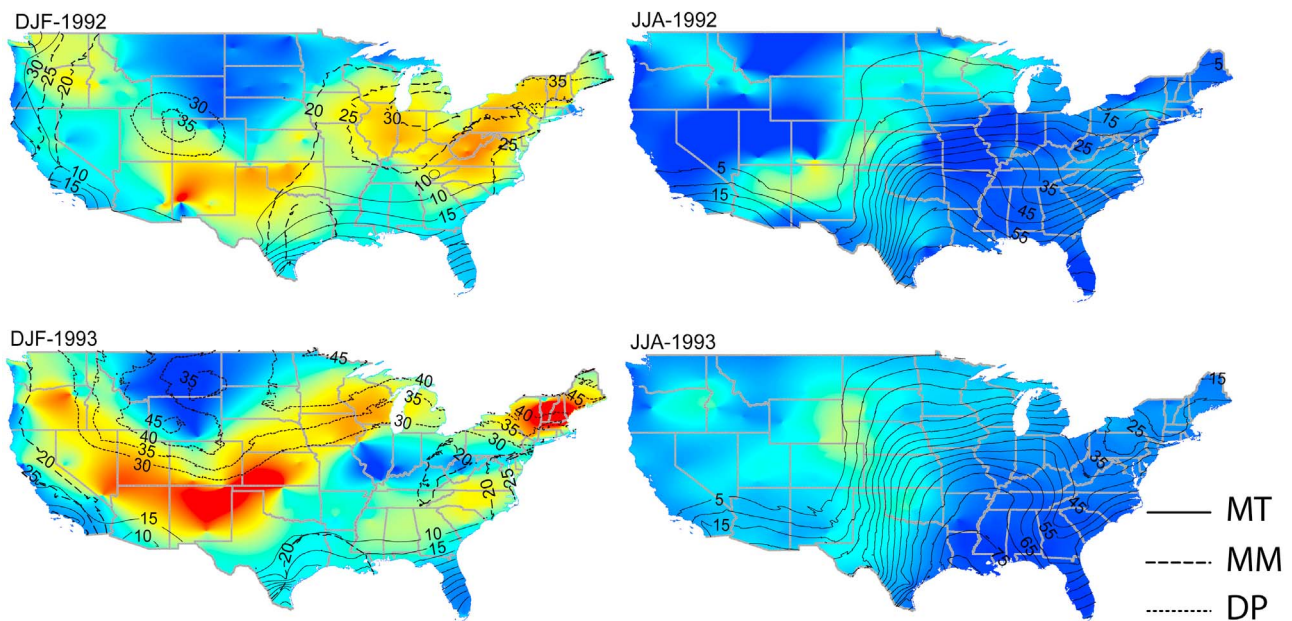


**Figure 11.** Air mass frequency for winter (DJF) and summer (JJA) of 1992 and 1993, based on the classifications of *Kalkstein et al.* [1996]. The frequency of the three dominant synoptic air masses are shown: dry polar (DP, analogous to traditional Continental Polar), moist moderate (MM, associated with overcast, humid conditions), and moist tropical (MT, analogous to traditional Maritime Tropical). Background color fields show the precipitation $\delta^{18}O$ slope values for each time period. The contour interval is 5%, with contours shown only for the upper range of frequency values for each air mass type.

[25] In contrast to summer season, winter climate over the contiguous United States features intensified and more dynamic interaction of moist tropical (MT), moist moderate (MM) and dry polar (DP) air masses (Figure 11). Previous work has demonstrated that precipitation originating from Arctic-derived air masses is characterized by very low $\delta^{18}O$ values, and the interaction of these systems with $^{18}O$-enriched vapor from tropical and midlatitude sources likely contributes to the higher mean and maximum $\delta^{18}O$ slope values during winter relative to summer (Figure 7). Across the western United States, the influence of DP air masses was much stronger in 1993 than in 1992, and the resultant strong gradients in air mass characteristics between coastal regions and the continental interior are closely matched by strong wintertime $\delta^{18}O$ gradients during 1993. During 1992, the relatively westerly position of wintertime high pressure (Figure 2) reduced the influence of both DP air masses in the interior and MT and MM air masses along the coast. As a result, this winter featured a reduction of land-falling Pacific storms and relatively dry conditions in coastal California, reduced precipitation amount gradients between the coast and interior, and diminished isotope gradients in this region (Figures 3, 4, and 11).

[26] East of the Rocky Mountains, a narrow and sharp transition zone between cool, dry continental air (dry polar, DP, air mass of *Kalkstein et al.* [1996]) and relatively warm, humid maritime air (moist moderate and moist tropical, MM and MT) occurs along the polar front (Figure 11) [*Lawrence et al.*, 1982]. During the winter season, this boundary coincides with the track of extratropical "Colorado cyclones" which lead to the convergence of maritime and polar air producing strong rainout [e.g., *Bierly and Winkler*, 2001; *Whittaker and Horn*, 1984]. The generalized path of these systems is well documented and corresponds closely to the geometry of the eastern branch of the high $\delta^{18}O$ slope trough observed in our study.

[27] The strength and position of this precipitation isotope slope feature varies slightly between the two study years, and is consistent with variation in the atmospheric circulation for these winters. During 1993, winter season high pressure in the continental interior was situated relatively far to the east, leading to a strong juxtaposition of DP and MT air masses along the Colorado cyclone track and promoting strong frontal precipitation across the central Great Plains and upper Midwest (Figures 2, 4, and 11). The resultant zone of high $\delta^{18}O$ slope values formed a strong and continuous band along the Colorado cyclone track. Due to the more westerly position of high-pressure systems during 1992, pressure gradients in the Great Plains and Midwest were reduced. Strong juxtaposition of DP and MT air masses was limited to the southern Great Plains and southern Rocky Mountains, and precipitation amounts in the area characterized by the Colorado cyclone were relatively low (Figures 2, 4, and 11). During this winter, the high $\delta^{18}O$ slope zone was of reduced magnitude and was discontinuous, with the highest slope values limited to the southern Rocky Mountain region where DP and MT air masses were most closely juxtaposed.

[28] During the winter of 1992, an additional zone of high $\delta^{18}O$ slopes occurs in the northeastern states, with a secondary branch extending south of the Great Lakes to Illi-

nois. This feature is noticeably diminished during the winter of 1993, although a small zone of very high slopes is located over the northeastern states and a secondary zone of moderately high slopes occurs farther to the south. This difference may also reflect the varying influence of different air masses and vapor sources throughout the region. The high $\delta^{18}O$ slopes in the region in 1992 approximately correspond to areas where the MM and MT air masses are juxtaposed. During winter of 1993, this interface is shifted southward and weaker, corresponding with the zone of moderately high $\delta^{18}O$ slopes in middle Atlantic Coast and southern Appalachians. The small zone of very high $\delta^{18}O$ slopes over the far northeastern states in 1993 separates areas strongly influenced by the DP and MM air masses.

[29] Another factor that may contribute to high $\delta^{18}O$ slopes in this region is the localized influence of the Great Lakes on precipitation in down-wind regions (lake effect). Previous work has demonstrated that evaporation of water from the Great Lakes is a significant source of water vapor contributing to winter season precipitation in areas downwind of the lakes and that the resultant precipitation is characterized by lower $\delta^{18}O$ values than precipitation from other vapor sources [*Gat et al.*, 1994; *Machavaram and Krishnamurthy*, 1994, 1995; *Burnett et al.*, 2004]. The formation of these lake-effect events is driven by destabilization of the overlying atmosphere by vertical fluxes of heat and recycled moisture from the lake surface, and as a result their occurrence is typically limited to a region within a few hundred kilometers of the lakes [*Niziol et al.*, 1995; *Burnett et al.*, 2004]. The position of the northeastern high $\delta^{18}O$ slope zone approximately corresponds with the expected maximum extent of lake-effect precipitation, and we suggest that high $\delta^{18}O$ gradients in this region may in part reflect the diminishing influence of the lake system with distance from the Lakes. Conditions during 1992 were optimal for expression of this contrast: a relatively dry winter with increased influence of MM air masses (potentially reflecting both Atlantic- and Great Lakes−influenced air masses as suggested by the two loci of high MM air mass frequency shown in Figure 11), decreased DP air mass influence, and slightly above average snowfall in lake effect areas (Figures 4 and 11) [*Burnett et al.*, 2003]. Conversely, the winter of 1993 was relatively wet across the region, with strong influence of DP air mass, potential for frontal precipitation across the region and relatively little enhancement of snowfall in lake-effect areas. These patterns suggest enhanced regional precipitation of moisture from maritime sources, potentially diluting the contrast between lake-effect and non-lake-effect areas and diminishing the $\delta^{18}O$ slopes across much of the northeastern United States.

## 5.4. Comparison With Deuterium Excess Pattern

[30] Although the deuterium excess values of precipitation are controlled by a complex of local and nonlocal processes, the spatial distribution of $d$ values can serve as a coarse tracer for water source given the strong influence of source-region conditions on the $d$ values of evaporated water [*Gat*, 1996]. Patterns of $d$ variation across the contiguous United States in two summers and winter of 1992 are in general agreement with the arguments presented so far for vapor-source controls on the patterns of $\delta^{18}O$ slopes (Figure 8).

During summer, low *d* values (<8‰) consistent with Pacific-sourced moisture [*Kendall and Coplen*, 2001] occur to the north and west of the steep $\delta^{18}$O slope band in the Great Plains, whereas sites to the south and east of the high-slope band are characterized by higher *d* values. Although the data are noisy and it is difficult to make a strong argument for robust differences between the summers, the interpolated patterns of *d* values for 1992 and 1993 suggest that variation in the spatial patterns may parallel variation in the orientation of the high $\delta^{18}$O slope bands for these summers. Winter precipitation *d* values in 1992 are consistent with a strong Pacific source influence across the northern interior of the continent, as suggested based on $\delta^{18}$O gradient analysis. During all seasons relatively high values of *d* in the northeastern states are consistent with some contribution of recycled water (e.g., from over-lake evaporation) to precipitation [*Gat et al.*, 1994].

## 6. Conclusion

[31] Spatial analysis of a dense network of precipitation isotope ratio monitoring sites across the contiguous United States indicates substantial variation in the rate and direction of change in isotope values over space, the precipitation isotope gradient, and suggests that the precipitation $\delta^{18}$O slope varies by an order of magnitude. This variation is spatially patterned and changes over time, with significant differences demonstrated here between summer and winter seasons and between equivalent seasons for two consecutive years. The patterns of $\delta^{18}$O gradients likely reflect a complex of factors that govern the moisture sources and rainout history of atmospheric vapor contributing to precipitation at different locations, but through analysis we are able to propose a suite of features of the atmospheric circulation that appear to influence the most significant features of the precipitation isotope gradient distributions. In summer, a north-south band of steep gradients in the isotope field along the Rocky Mountain front corresponds approximately to zone of convergence of Pacific and the Gulf of Mexico air masses as defined by the strength and position of low-pressure systems over the Great Plains. During 1993, when strong northwestward transport of Gulf moisture brought flooding to the upper Midwest and northern Great Plains states, the band of steep $\delta^{18}$O gradients retreated to the north and west compared to the summer of 1992, when steep gradients extended across this region. During winter, the zone of high isotope gradients encloses the Rocky Mountains and northern Great Plains, reflecting the influence of the polar front and presence of blocking high-pressure systems and cyclone tracks across this region. The west-shifted position of continental high pressure during the winter of 1992 corresponded with a reduction in land-falling Pacific storms in the southwestern United States and diminished winter season isotope gradients. During 1993, the wintertime high-pressure center was situated farther east over the Great Plains, promoting frontal precipitation and cyclogenesis in the Great Plains and Midwest, increasing the cyclonic transport of Gulf and Atlantic moisture to the continental interior, and intensifying the precipitation isotope gradients in the Great Plains and Midwest while diminishing those surrounding the Great Lakes "lake-effect" region.

[32] The recognition that circulation and vapor-source patterns are reflected in precipitation isotope gradient fields at continental scales presents a number of opportunities for studying the modern atmospheric and land-atmosphere components of the water cycle. Water vapor transport and mixing have been modeled extensively but are extremely difficult to verify observationally. Moreover, there is significant concern that anthropogenic land use change and climate change are significantly modifying these processes [e.g., *Betts et al.*, 2007; *Zhang et al.*, 2007]. Recent advances in technology promise to enable routine regional- to continental-scale monitoring of atmospheric water vapor isotopic composition from satellite and ground-based platforms within the next decade [*Helliker and Noone*, 2010]. The spatial gradient analysis proposed here represents a simple method that could be applied to the resultant data to derive first-order information about atmospheric and land-atmosphere moisture fluxes and test models for these processes, and could easily be adopted as a routine data analysis method in atmospheric and precipitation isotope monitoring efforts.

[33] Within the paleoclimate field, isotope archive records from individual sites have been widely useful in reconstructing time series for local paleoclimate variables, but in order to better understand past climate and the relationships between climate dynamics and climate change impacts, researchers need to be able to reconstruct synoptic and dynamic features of climate that are defined by their spatial structure [e.g., *Shinker et al.*, 2006]. Such reconstructions may be obtained from single-site records where relationships between local climate and large-scale features are especially robust, but a less ambiguous approach would involve direct reconstruction of the spatial patterns themselves. This study demonstrates relationships between the spatial structure of precipitation isotopes and aspects of the modern atmospheric circulation over the contiguous United States. Our work suggests that changes in these features of the synoptic circulation, and in likelihood other similar features occurring elsewhere in the world, could be directly reconstructed based on spatially distributed networks of isotope archive records. Until recently the recovery of archive records required to support interpretations based on spatial analysis has been prohibitive, but advances in analytical methodology and recent examples from lacustrine and tree ring research suggest that this may no longer be the case [e.g., *Feng et al.*, 2007]. If so, spatial analysis of isotope archive data may produce new, more direct records of past atmospheric circulation and large-scale climate features, supporting an improved understanding of past climate states and climate change impacts.

## References

Adler, R. F., et al. (2003), The version-2 global precipitation climatology project (GPCP) monthly precipitation analysis (1979–present), *J. Hydro-*

*meteorol.*, *4*, 1147–1167, doi:10.1175/1525-7541(2003)004<1147: TVGPCP>2.0.CO;2.

Amundson, R., et al. (1996), Isotopic evidence for shifts in atmospheric circulation patterns during the late Quaternary in mid-North America, *Geology*, *24*(1), 23–26, doi:10.1130/0091-7613(1996)024<0023:IEFSIA> 2.3.CO;2.

Anderson, L., et al. (2001), Holocene climate inferred from oxygen isotope ratios in lake sediments, central Brooks Range, Alaska, *Quat. Res.*, *55*(3), 313–321, doi:10.1006/qres.2001.2219.

Baldini, L. M., F. McDermott, A. M. Foley, and J. U. L. Baldini (2008), Spatial variability in the European winter precipitation $\delta^{18}$O-NAO relationship: Implications for reconstruction NAO-mode climate variability in the Holocene, *Geophys. Res. Lett.*, *35*, L04709, doi:10.1029/ 2007GL032027.

Betts, R. A., et al. (2007), Projected increase in continental runoff due to plant responses to increasing carbon dioxide, *Nature*, *448*(7157), 1037–1041, doi:10.1038/nature06045.

Bierly, G. D., and J. A. Winkler (2001), A composite analysis of airstreams within cold-season Colorado cyclones, *Weather Forecast.*, *16*(1), 57–80, doi:10.1175/1520-0434(2001)016<0057:ACAOAW>2.0.CO;2.

Birks, S. J., and T. W. D. Edwards (2009), Atmospheric circulation controls on precipitation isotope-climate relations in western Canada, *Tellus, Ser. B*, *61*, 566–576, doi:10.1111/j.1600-0889.2009.00423.x.

Bowen, G. J. (2008), Spatial analysis of the intra-annual variation of precipitation isotope ratios and its climatological corollaries, *J. Geophys. Res.*, *113*, D05113, doi:10.1029/2007JD009295.

Bowen, G. J., and B. Wilkinson (2002), Spatial distribution of $\delta^{18}$O in meteoric precipitation, *Geology*, *30*(4), 315–318, doi:10.1130/0091-7613(2002)030<0315:SDOOIM>2.0.CO;2.

Bryson, R. A., and R. K. Hare (1974), The climate of North America, in *Climates of North America*, *World Surv. Climatol.*, vol. 11, pp. 1–47, Elsevier, New York.

Burnett, A. W., et al. (2003), Increasing Great Lake–effect snowfall during the Twentieth Century: A regional response to global warming?, *J. Clim.*, *16*, 3535-3542, doi:10.1175/1520-0442(2003)016<3535:IGLSDT>2.0. CO;2.

Burnett, A. W., H. T. Mullins, and W. P. Patterson (2004), Relationship between atmospheric circulation and winter precipitation $\delta^{18}$O in central New York State, *Geophys. Res. Lett.*, *31*, L22209, doi:10.1029/ 2004GL021089.

Dorale, J. A., et al. (1992), A high-resolution record of Holocene climate change in speleothem calcite from Cold Water Cave, northeast Iowa, *Science*, *258*(5088), 1626–1630, doi:10.1126/science.258.5088.1626.

Dorale, J. A., et al. (1998), Climate and vegetation history of the midcontinent from 75 to 25 ka: A speleothem record from Crevice Cave, Missouri, USA, *Science*, *282*(5395), 1871–1874, doi:10.1126/science. 282.5395.1871.

Dutton, A., et al. (2005), Spatial distribution and seasonal variation in $^{18}$O/$^{16}$O of modern precipitation and river water across the conterminous USA, *Hydrol. Processes*, *19*(20), 4121–4146, doi:10.1002/hyp.5876.

Feng, X. H., et al. (2007), The changes in North American atmospheric circulation patterns indicated by wood cellulose, *Geology*, *35*(2), 163–166, doi:10.1130/G22884A.1.

Fricke, H. C., and J. R. O'Neil (1999), The correlation between $^{18}$O/$^{16}$O ratios of meteoric water and surface temperature: Its use in investigating terrestrial climate change over geologic time, *Earth Planet. Sci. Lett.*, *170*, 181–196, doi:10.1016/S0012-821X(99)00105-3.

Friedman, I., J. M. Harris, G. I. Smith, and C. A. Johnson (2002a), Stable isotope composition of waters in the Great Basin, United States: 1. Airmass trajectories, *J. Geophys. Res.*, *107*(D19), 4400, doi:10.1029/ 2001JD000565.

Friedman, I., G. I. Smith, C. A. Johnson, and R. J. Moscati (2002b), Stable isotope compositions of waters in the Great Basin, United States: 2. Modern precipitation, *J. Geophys. Res.*, *107*(D19), 4401, doi:10.1029/ 2001JD000566.

Gat, J. R. (1996), Oxygen and hydrogen isotopes in the hydrologic cycle, *Annu. Rev. Earth Planet. Sci.*, *24*, 225–262.

Gat, J. R., C. J. Bowser, and C. Kendall (1994), The contribution of evaporation from the Great Lakes to the continental atmosphere: Estimate based on stable isotope data, *Geophys. Res. Lett.*, *21*(7), 557–560, doi:10.1029/94GL00069.

Harvey, F. E., and J. M. Welker (2000), Stable isotopic composition of precipitation in the semi-arid north-central portion of the US Great Plains, *J. Hydrol.*, *238*, 90–109, doi:10.1016/S0022-1694(00)00316-4.

Helliker, B. R., and D. Noone (2010), Novel approaches for monitoring of water vapor isotope ratios: Plants, lasers and satellites, in *Isoscapes*, pp. 71–88, Elsevier, New York.

Ingraham, N. L., and B. E. Taylor (1991), Light stable isotope systematics of large-scale hydrologic regimes in California and Nevada, *Water Resour. Res.*, *27*(1), 77–90, doi:10.1029/90WR01708.

Ingraham, N. L., et al. (1991), Stable isotopic study of precipitation and spring discharge in southern Nevada, *J. Hydrol.*, *125*, 243–258, doi:10.1016/0022-1694(91)90031-C.

Joussaume, S., and J. Jouzel (1993), Paleoclimatic tracers: An investigation using an atmospheric general circulation model under ice age conditions: 2. Water isotopes, *J. Geophys. Res.*, *98*, 2807–2830, doi:10.1029/ 92JD01920.

Kalkstein, L. S., et al. (1996), A new spatial synoptic classification: Application to air-mass analysis, *Int. J. Climatol.*, *16*(9), 983–1004, doi:10.1002/(SICI)1097-0088(199609)16:9<983::AID-JOC61>3.0. CO;2-N.

Kendall, C., and T. B. Coplen (2001), Distribution of oxygen-18 and deuterium in river waters across the United States, *Hydrol. Processes*, *15*(7), 1363–1393, doi:10.1002/hyp.217.

Kohn, M. J., and J. M. Welker (2005), On the temperature correlation of $\delta^{18}$O in modern precipitation, *Earth Planet. Sci. Lett.*, *231*(1–2), 87–96, doi:10.1016/j.epsl.2004.12.004.

Lawrence, J. R., et al. (1982), Storm trajectories in eastern US D/H isotopic composition of precipitation, *Nature*, *296*(5858), 638–640, doi:10.1038/ 296638a0.

Machavaram, M. V., and R. V. Krishnamurthy (1994), Survey of factors controlling the stable isotope ratios in precipitation in the Great Lakes region, USA, *Isr. J. Earth Sci.*, *43*, 195–202.

Machavaram, M. V., and R. V. Krishnamurthy (1995), Earth surface evaporative process: A case study from the Great Lakes region of the United States based on deuterium excess in precipitation, *Geochim. Cosmochim. Acta*, *59*(20), 4279–4283, doi:10.1016/0016-7037(95)00256-Y.

Maglaras, G. J., et al. (1995), Winter weather forecasting throughout the eastern United States. Part I: An overview, *Weather Forecast.*, *10*(1), 5–20, doi:10.1175/1520-0434(1995)010<0005:WWFTTE>2.0.CO;2.

Moyeed, R. A., and A. Papritz (2002), An empirical comparison of kriging methods for nonlinear spatial point prediction, *Math. Geol.*, *34*(4), 365–386, doi:10.1023/A:1015085810154.

Niziol, T. A., et al. (1995), Winter weather forecasting throughout the eastern United States. Part IV: Lake effect snow, *Weather Forecast.*, *10*(1), 61–77, doi:10.1175/1520-0434(1995)010<0061:WWFTTE>2.0.CO;2.

Rozanski, K., et al. (1992), Relation between long-term trends of O-18 isotope composition of precipitation and climate, *Science*, *258*(5084), 981–985, doi:10.1126/science.258.5084.981.

Rozanski, K., L. Araguas-Araguas, and R. Gonfiantini (1993), Isotopic patterns in modern global precipitation, in *Climate Change in Continental Isotopic Records*, *Geophys. Monogr. Ser.*, vol. 78, edited by P. K. Swart et al., pp. 1–36, AGU, Washington, D. C.

Schwalb, A., and W. E. Dean (2002), Reconstruction of hydrological changes and response to effective moisture variations from north-central USA lake sediments, *Quat. Sci. Rev.*, *21*(12–13), 1541–1554, doi:10.1016/S0277-3791(01)00121-4.

Sheridan, S. C. (2002), The redevelopment of a weather-type classification scheme for North America, *Int. J. Climatol.*, *22*(1), 51–68, doi:10.1002/ joc.709.

Shinker, J. J., et al. (2006), Synoptic and dynamic climate controls of North American mid-continental aridity, *Quat. Sci. Rev.*, *25*(13–14), 1401–1417, doi:10.1016/j.quascirev.2005.12.012.

Sjostrom, D. J., and J. M. Welker (2009), The influence of air mass source on the seasonal isotopic composition of precipitation, eastern USA, *J. Geochem. Explor.*, *102*(3), 103–112, doi:10.1016/j.gexplo.2009.03.001.

Smith, M. A., and D. J. Hollander (1999), Historical linkage between atmospheric circulation patterns and the oxygen isotopic record of sedimentary carbonates from Lake Mendota, Wisconsin, USA, *Geology*, *27*(7), 589–592, doi:10.1130/0091-7613(1999)027<0589:HLBACP>2.3.CO;2.

Vachon, R. W., J. W. C. White, E. Gutmann, and J. M. Welker (2007), Amount-weighted annual isotopic ($\delta^{18}$O) values are affected by the seasonality of precipitation: A sensitivity study, *Geophys. Res. Lett.*, *34*, L21707, doi:10.1029/2007GL030547.

Welker, J. M. (2000), Isotopic ($\delta^{18}$O) characteristics of weekly precipitation collected across the USA: An initial analysis with application to water source studies, *Hydrol. Processes*, *14*(8), 1449–1464, doi:10.1002/ 1099-1085(20000615)14:8<1449::AID-HYP993>3.0.CO;2-7.

Whittaker, L. M., and L. H. Horn (1984), Northern Hemisphere extratropical cyclone activity for four mid-season months, *Int. J. Climatol.*, *4*(3), 297–310, doi:10.1002/joc.3370040307.

Wright, W. E., and S. W. Leavitt (2006), Boundary layer humidity reconstruction for a semiarid location from tree ring cellulose $\delta^{18}$O, *J. Geophys. Res.*, *111*, D18105, doi:10.1029/2005JD006806.

Yoshimura, K., M. Kanamitsu, D. Noone, and T. Oki (2008), Historical isotope simulation using Reanalysis atmospheric data, *J. Geophys. Res.*, *113*, D19108, doi:10.1029/2008JD010074.

Yu, Z., and U. Eicher (1998), Abrupt climate oscillations during the last deglaciation in central North America, *Science*, *282*(5397), 2235–2238, doi:10.1126/science.282.5397.2235.

Yu, Z. C., et al. (1997), Middle Holocene dry climate caused by change in atmospheric circulation patterns: Evidence from lake levels and stable isotopes, *Geology*, *25*(3), 251–254, doi:10.1130/0091-7613(1997)025<0251:MHDCCB>2.3.CO;2.

Zhang, X. B., et al. (2007), Detection of human influence on twentieth-century precipitation trends, *Nature*, *448*(7152), 461–464, doi:10.1038/nature06025.

G. J. Bowen and Z. Liu, Department of Earth and Atmospheric Sciences, Purdue University, 550 Stadium Mall Dr., West Lafayette, IN 47907, USA. (gabe@purdue.edu)

J. M. Welker, Environment and Natural Resources Institute, University of Alaska Anchorage, 707 A St., Anchorage, AL 99501, USA.